FERMILAB-CONF-05-008-AD

Beam-beam Simulations of Hadron Colliders

Tanaji Sen
Fermilab, PO Box 500, Batavia, IL 60510

Abstract

Simulations of beam-beam phenomena in the Tevatron and RHIC as well as for the LHC are reviewed. The emphasis is on simulations that can be closely connected to observations.

I. INTRODUCTION

Beam-beam phenomena have been studied intensively ever since the first storage ring collider started operation. These interactions have limited the achievable luminosity and beam intensities in both hadron and lepton colliders. However the nature of the limitations in these two classes of colliders is sufficiently different that distinctly different analytic and simulation tools have been developed. In this review I will focus on recent developments in beam-beam simulations for hadron colliders. The emphasis will be on connecting simulation results to observations; almost nothing will be said about the simulation techniques.

II. USES OF SIMULATIONS

Simulations of beam dynamics can be useful for different reasons. At the design stage of an accelerator they can be useful in guiding the proper choice of beam and machine parameters. Examples would be the several simulations done for the LHC. Historically this has been the most important contribution of simulations. Simulations can also be useful in understanding beam observations in existing accelerators. I will present several examples for the Tevatron later in this report. Finally, simulations could be used to improve the performance of an existing accelerator. This is perhaps the most demanding requirement. To date there are few examples of beam-beam simulations of hadron colliders having been useful in this respect. This situation is changing due to advances in physics modeling and computing power. The easier availability of parallel computing makes it possible to include more details of an accelerator in the simulation model. It is also easier to calculate those beam parameters that are routinely measured in every store but are computationally demanding, such as emittances and lifetimes.

III. HADRON COLLIDERS

I will consider beam-beam phenomena in the two existing hadron colliders Tevatron and RHIC as well as the future LHC. HERA is a hybrid (a lepton-hadron collider) and interesting beam-beam observations have been reported recently [1]. However the phenomena appear to be closely connected to the dynamics of the lepton beam.

In the Tevatron, protons and anti-protons circulate within the same beam pipe and collide at two interaction points (IPs) B0 and D0. The ratio of anti-proton intensities to proton intensities is about 1:7 at present, thus the beam-beam phenomena are in the classical “weak-strong” regime. Nonetheless we observe that anti-protons do influence the protons. At injection energy, both beams experience only long-range interactions while at collision there are two head-on collisions and seventy long-range interactions per bunch. These interactions limit beam lifetimes at all stages of the Tevatron’s operational cycle. RHIC collides polarized protons and at other times, heavy ions such as gold. Both beams have similar intensities and the beam-beam phenomena are in the classical “strong-strong” regime. There are two rings and typically each bunch experiences 4 head-on collisions and 2 long-range interactions. Coherent modes excited by these collisions have been observed in RHIC. The LHC will collide proton beams of equal intensities at two high luminosity IPs and also at two low luminosity IPs. Beam-beam phenomena there will be in the “strong-strong” regime. In addition, each bunch experiences several long-range interactions around each IP. These interactions are expected to hurt beam quality and several simulations have addressed their expected impact. Compensation of these long-range beam-beam interactions with wires

has been proposed for the LHC and initial tests with wires acting on a single beam in the SPS have been carried out. Plans are now underway to test this principle in an existing collider with two beams.

IV. SIMULATION CODES

Until recently most hadron collider beam-beam simulation codes were used to calculate tune shifts with amplitude and dynamic apertures (DAs). These quantities are only measured in dedicated beam studies. In recent years several weak-strong simulation codes have been written to calculate quantities that are routinely observed such as emittances and lifetimes. Strong-strong codes typically calculate the mode spectrum and also emittance changes. Table I lists some of the simulation codes and their purpose.

The codes used at FNAL for lifetime calculations are all parallelized codes. DA codes are typically single processor codes but can be "trivially" parallelized. The references should be consulted for more details on these codes.

Simulation Code	Purpose
FNAL	
BBSIM [2], LIFETRAC [3], PLIBB [4], BEAMBEAM3D [5]	Lifetime calculations
MAD [6], SIXTRACK [7], TEVLAT [8]	Dynamic aperture
RHIC	
BBDEMO2C [9], BEAMBEAM3D	Coherent modes
LHC	
WSDIFF [10], SIXTRACK, MAD	Diffusion, Dynamic aperture
BEAMX [11], COMBI, BEAMBEAM3D	Coherent modes

Table 1: Beam-beam simulation codes. The numbers in [] are the reference numbers.

V. TEVATRON: OBSERVATIONS & SIMULATIONS

Beam-beam interactions have limited the performance of the Tevatron since the start of Run II in 2001. Several improvements have significantly reduced the beam loss due to these interactions. At present the performance limitations are not severe but there are observable influences due to these interactions. See reference [12] for a discussion of beam-beam phenomena in the Tevatron. Here I will choose some observations that have been qualitatively reproduced in simulations.

In early 2003 the Tevatron was operated without transverse dampers but at high chromaticity in order to keep the beams stable. At injection energy, typical chromaticities were about 8 units in both planes. During this period we observed a strong reduction in the anti-proton emittances soon after they were injected.

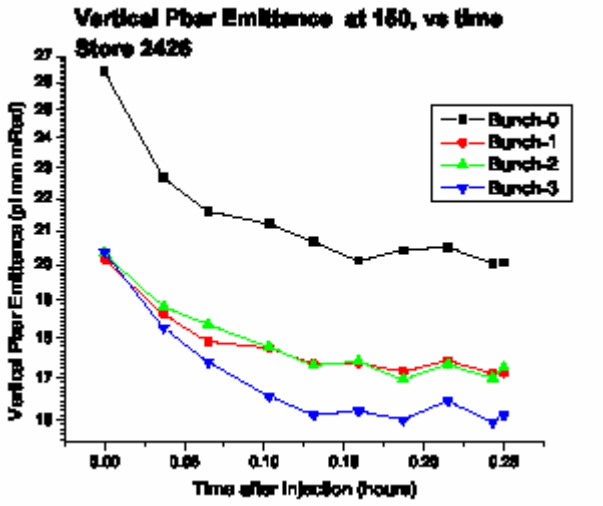

Figure 1: Emittances of anti-protons after injection (April 2003)

Figure 1 shows the emittance of 4 anti-proton bunches measured with flying wires 10 times at injection energy during a store in April 2003. These 4 bunches were injected first among the 36 bunches enabling several measurements of their emittance. The emittance of all bunches fell sharply right after injection before reaching an asymptotic value during this time of 15 minutes that the beams were at injection energy. The same phenomenon was observed in several stores in April 2003. This occurred because the DA was much smaller than the initial beam width. Beam outside the DA was lost; the emittance fell until the beam was small enough to fill the DA.

The DA extracted from these measurements over several stores for the 4 bunches is shown in Figure 2. The measured DA varied from 3.5-4 σ for these bunches. The error bars represent the variations over the measurements. The dynamic aperture was

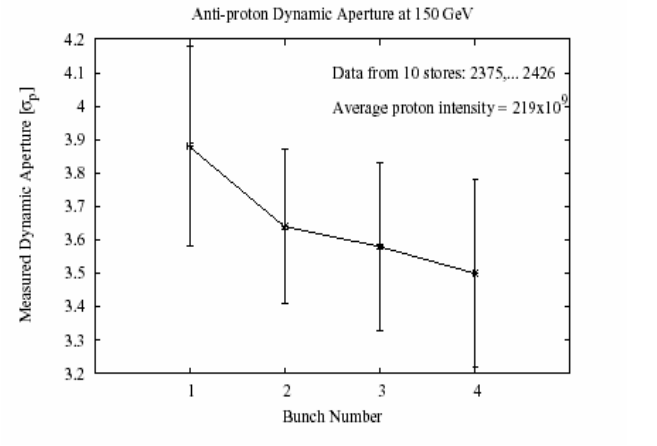

Figure 2: Dynamic aperture extracted from emittance measurements in April 2003.

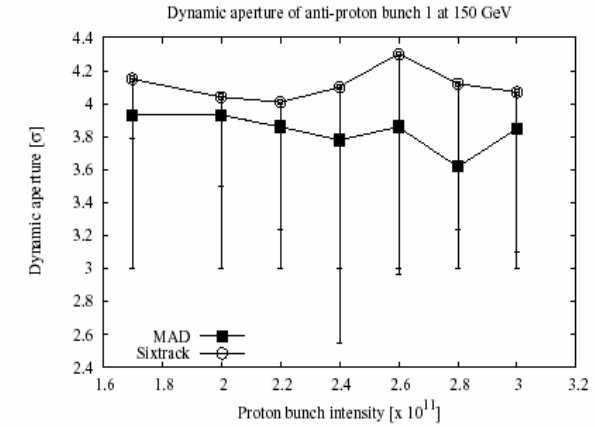

Figure 3: Dynamic aperture from simulations for the conditions in Figure 2.

calculated with the programs Sixtrack and Mad. The simulation model included the known multipole moments in all the arc magnets but not the alignment errors. Chromaticities were set to 8 units in both planes. The expected differences between the model optics and the real machine optics are about 20%. Figure 3 shows the calculated DAs as a function of proton intensity. Despite the differences between the model and the machine optics, the DAs calculated by both codes were around 4 σ at the proton intensities in the machine – close to the measured values. The impact of the nonlinearities was strong enough that the inaccuracies of the linear optics were less important. The agreement between calculations and measurements was not as good at smaller values of the chromaticity. The calculated DAs fell relatively slowly with chromaticity while measurements at chromaticities of (4,2) units (after dampers were operational) showed no reduction in the initial emittance implying that the DA was significantly greater than the values shown in Figure 2.

Several codes were used to calculate anti-proton lifetimes at injection where the measured lifetime is a few hours. The statistical accuracy from a numerical estimation of a 1hr lifetime in the Tevatron is ~10% if more than $2x10^{10}$ particle-turns are used. If all the multipole moments in the magnets are included in a simulation model, the computational time required for tracking these many particle-turns is prohibitively large even with the use of multiple processors. Lifetime simulations at injection have therefore included only the beam-beam nonlinearities.

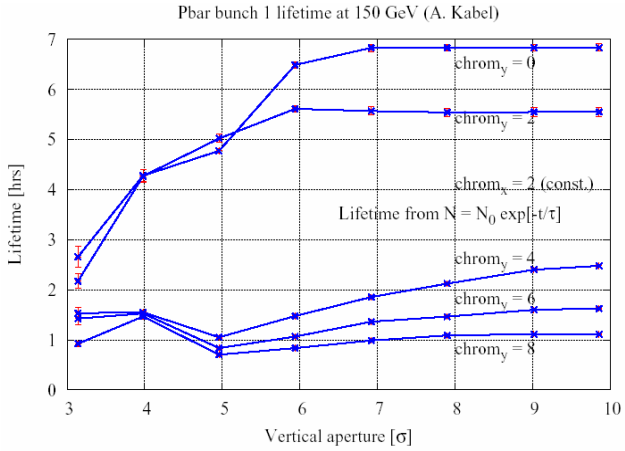

Figure 4: Anti-proton bunch lifetime vs. vertical aperture at different values of the vertical chromaticity (courtesy A. Kabel).

The dependence of the lifetime on the vertical chromaticity was calculated with the code PlibB [4] since observations showed that the lifetime was very sensitive to this parameter. Figure 4 shows the calculated lifetime for anti-proton bunch 1 at injection as a function of the vertical aperture for

different values of the vertical chromaticity. The horizontal chromaticity was fixed at 2 units. At vertical chromaticities ≥ 4 units, the lifetimes are in the range of 1-2.5 hrs and are not very sensitive to the aperture. But at chromaticities ≤ 2 units, the lifetime increases sharply as the aperture increases from 3 to 6 σ before leveling off. The physical aperture at injection is ~6σ - it is interesting that the simulation predicts a significant jump in lifetime as the chromaticity is lowered from 4 to 2 units. Once the transverse dampers were commissioned in the Tevatron, the chromaticities were lowered to (4,2) units and the anti-proton lifetime improved to an average of around 5 hrs at injection.

After both beams are loaded, they are accelerated to 980 GeV in about 84 seconds. There are beam losses during this stage, typically less than 10%. Dedicated machine studies have shown that proton losses during acceleration are not affected by anti-protons while the anti-proton losses increase in the presence of the protons. So far no simulations have been performed to follow the acceleration process, mainly because the losses are typically small.

After reaching flat top, the optics is changed to reduce the β* at B0 and D0 to 0.35m. In the early stages of Run II there were large anti-proton losses between 10-25% during the portion of the beta squeeze when the helices changed polarities. The minimum separation had dropped to less than 2 σ at this point. When the separator voltages were changed to increase the minimum beam separation to more than 3.5 σ, anti-proton losses also dropped significantly. Now beam losses during the squeeze are typically no more than 2%.

After the beams are brought to collision, the beams experience head-on interactions and long-range interactions. Observations show that both protons and anti-protons are influenced by the other beam. The long store times during collision allow detailed beam observations that cannot be made during injection. At 980 GeV, there is enough synchrotron radiation light to image the two beams in a synchrotron light monitor.

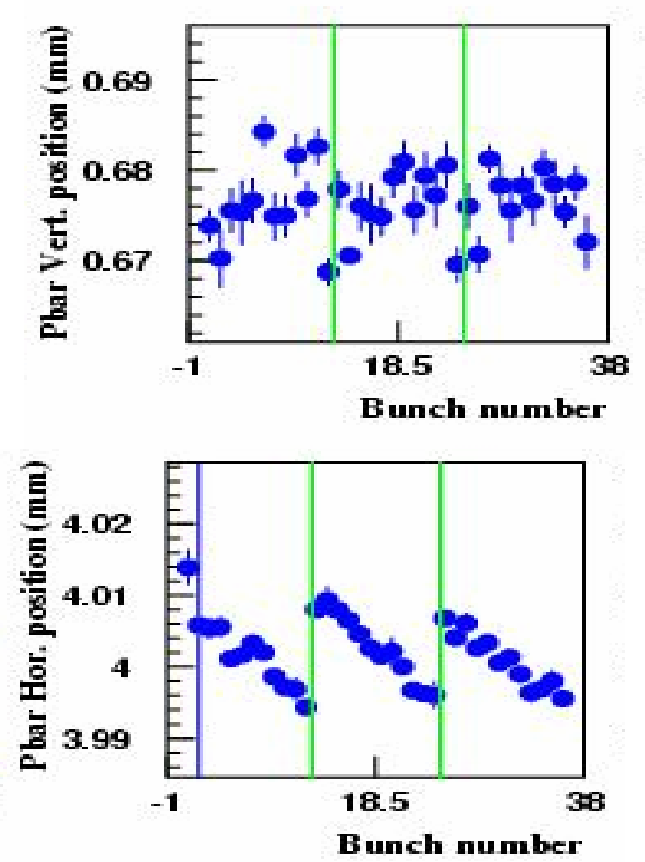

Figure 5: Bunch by bunch orbits (top: hor., bottom: vert.) of anti-protons observed during a store at the synchrotron light monitor.

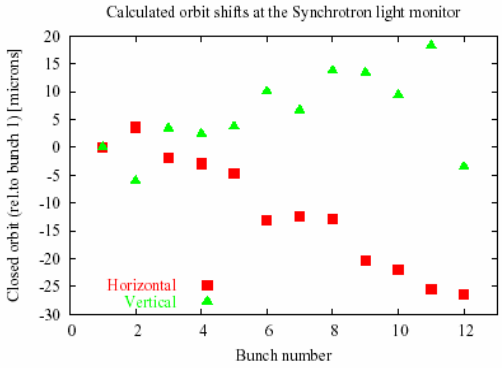

Figure 6: Calculated bunch by bunch orbits of anti-protons

Figures 5 and 6 show the observed and calculated bunch-by-bunch orbits of anti-protons at the synchrotron light monitor. The calculated orbits reproduce the different patterns of the horizontal and vertical orbits as well as the scale of the orbit shifts.

The commissioning of a high frequency 1.7 GHz Schottky monitor has enabled the measurement of bunch-by-bunch tunes during stores – see Reference [13]. Signals are gated in order to acquire the data from individual bunches and so far the bunch by bunch tunes of either anti-protons or protons have been measured in a single store.

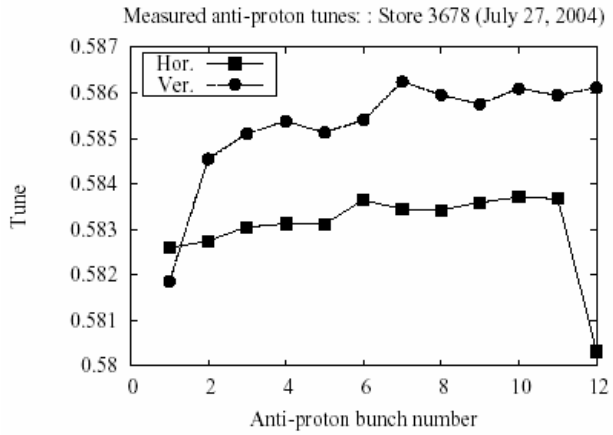

Figure 7: Measured anti-proton tunes bunch by bunch.

The pattern of measured tunes, a representative sample for a particular store is seen in Figure 7, is reproduced in different stores. The calculated anti-proton tunes, see Reference [14], agree reasonably well with the measured values.

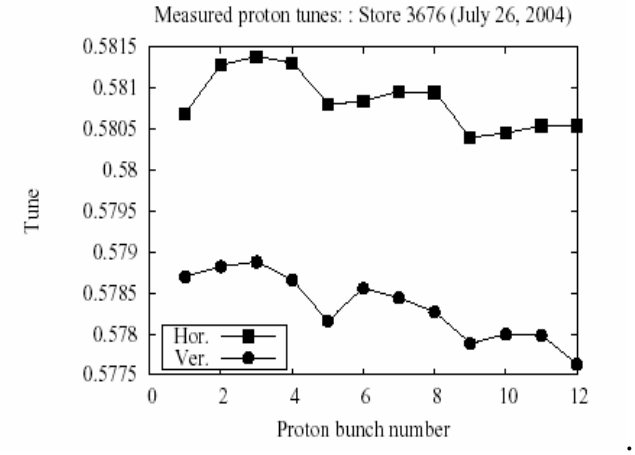

Figure 8: Measured proton tunes bunch by bunch in a store.

Figure 8 shows an example of measured proton tunes bunch-by-bunch. The differences in tunes between proton bunches is also due to beam-beam effects from the anti-protons - the observed pattern follows the variation in anti-proton bunch intensities.

Emittance growth of anti-protons also varies from bunch to bunch. Until the fall of 2004 it was observed that the emittance growth of the head and tail bunches in a train of 12 bunches was smaller than that of other bunches - giving a scalloped shape to the emittance profile.

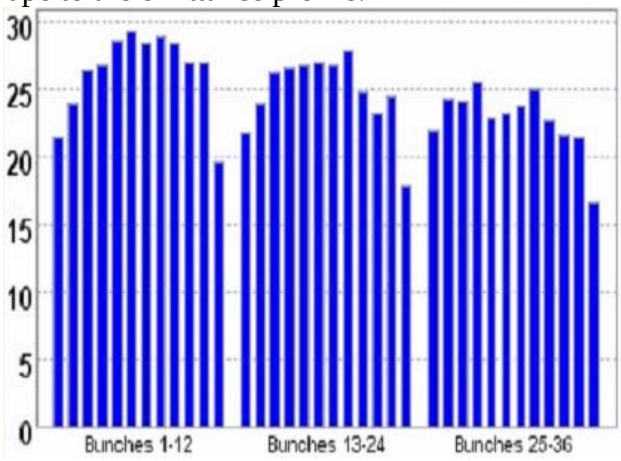

Figure 9: Vertical emittance profile of anti-proton bunches soon after the start of a store.

An example of this scalloped profile can be seen in Figure 9. The rapid emittance growth of most bunches results in a significant luminosity loss. Empirically the problem has been solved by small changes in the tunes. The Tevatron electron lens was used successfully on one occasion to reduce the emittance growth of a selected bunch [15].

Simulations have attempted to understand the sensitive dependence of the emittance growth on the tunes. An example using the code LIFETRAC is seen in Figure 10. Lowering the horizontal tune by 0.005 reduces the emittance growth of most bunches – roughly in accord with observations. – while the emittance of the last bunch grows more rapidly. The scalloped profile is not seen in the profile at the higher tune but nevertheless the simulation does demonstrate the tune dependence of emittance growth.

Beam lifetimes also show strong variations from bunch to bunch. These lifetimes depend on the beam parameters such as the intensities and emittances. Proton bunch intensities and emittances vary by about 10% across all 36 bunches.

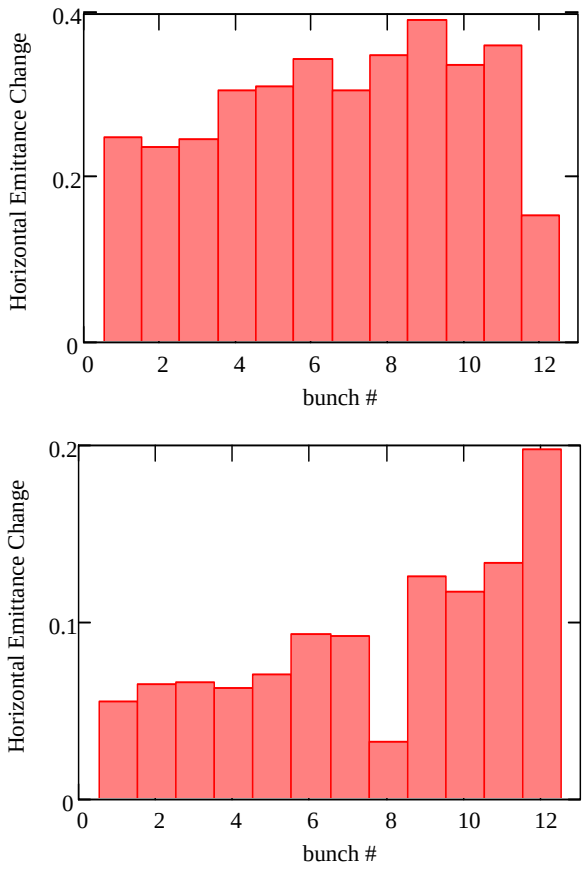

Figure 10: Horizontal emittance growth of anti-proton bunches calculated using LIFETRAC. Top: tunes are (0.585, 0.575); Bottom: tunes are (0.580, 0.575) - courtesy of A. Valishev.

As an illustration we consider beam parameters during a store on July 16, 2004 when the highest luminosity of 1.3×10^{32} cm^{-2} sec^{-1} was recorded in the Tevatron. Figure 11 shows the proton intensities and emittances over all bunches – the largest variations are in the first 3 or 4 bunches at the head of each train. There was a 10% variation in proton intensities with an average intensity ~250×10^9. The average horizontal and vertical emittances were 20 and 13 πmm-mrad respectively with a similar 10% variation in each plane over all bunches.

The variation in anti-proton parameters is considerably greater. Figure 12 shows that the anti-proton bunch intensities and emittances varied by a factor of 2 or more in the same store.

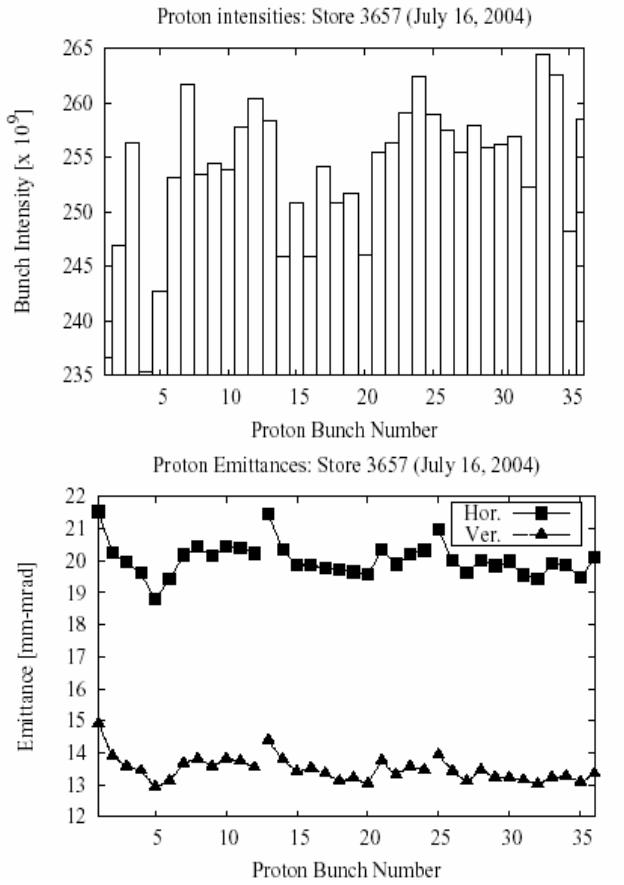

Figure 11: Proton intensities (top) and emittances (bottom) at the start of the store on July 16, 2004

The ratio of proton to anti-proton bunch intensities varied in the range from 4 to 10. Anti-proton bunch emittances are largely determined by the length of time spent circulating in the Accumulator where they are stochastically cooled. These bunches are injected four at a time into the Tevatron. Consequently the last four bunches to be injected typically have the smallest emittances.

These large variations in anti-proton bunch parameters naturally lead to large variations in the bunch luminosities, given approximately by

$$L = \frac{f_{rev} N_p N_A}{4\pi\beta^* \varepsilon} H\left(\frac{\beta^*}{\sigma_s}\right)$$

where f_{rev} is the revolution frequency, N_p and N_A are the proton and antiproton bunch intensities of the colliding bunches and H is the hourglass factor.

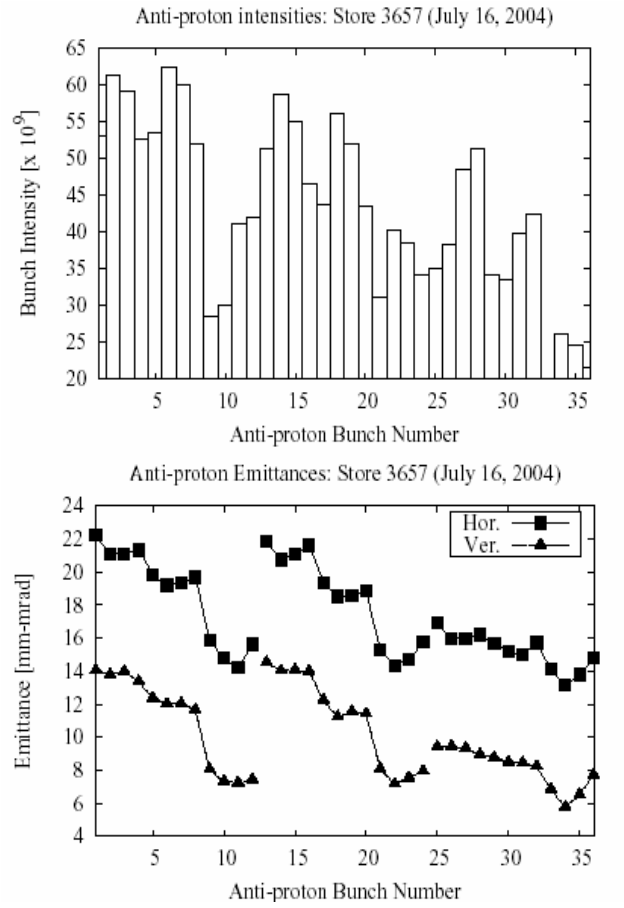

Figure 12: Anti-proton bunch intensities (top) and emittances (bottom) in the July 16, 2004 store.

Beam lifetimes can be usefully split into two contributions: the dominant one from luminosity and the other from dynamic processes unrelated to luminosity such as beam-beam effects, intra-beam scattering, gas scattering etc. To isolate the lifetime due to dynamic processes, we remove the contribution of the luminosity lifetime as

$$\frac{1}{\tau_{Dyn}} = \frac{1}{\tau_{Beam}} - \frac{1}{\tau_{Lum}}$$

and the luminosity lifetime for an antiproton bunch for example is

$$\frac{1}{\tau_{Lum,A}} = \frac{L\Sigma_{pA}}{N_A}$$

Here Σ_{pA} is the inelastic proton-antiproton scattering cross-section, assumed to be 70 mbarns at 980 GeV. The luminosity lifetime of an antiproton bunch is independent of the intensity of that bunch.

The bunch-by-bunch dynamic lifetimes τ_{Dyn} are shown in Figure 13 for the July 16, 2004 store and for another store on August 18, 2004. The bunch intensities and emittances for the later store can be seen in Reference [12].

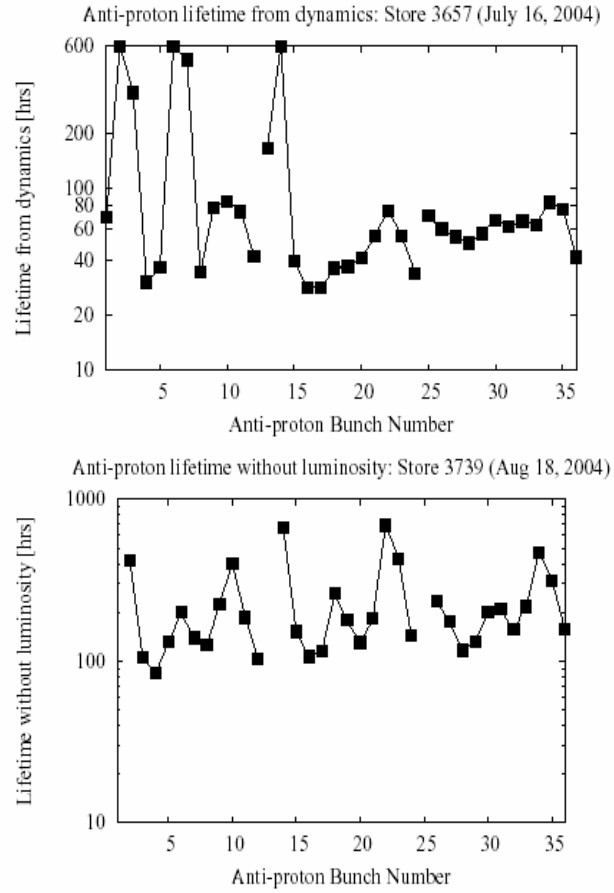

Figure 13: Anti-proton lifetime due to dynamics during the 1st two hours in two different stores. Top: July 16, 2004, Bottom: August 18, 2004

There is no obvious 3-fold symmetry in these lifetimes between the bunch trains in the July 16th store but there is such an approximate symmetry in the August 18th store. These dynamic lifetimes vary by more than a factor of 10 between bunches – the dominant sources of these differences are the beam-beam interactions. A powerful test of the simulations would be to reproduce these relative variations. Absolute calculations of lifetimes in this range of 10s – 100s of hours are meaningless at present because statistical errors are very large with the computing resources available.

As a first attempt we have calculated the lifetimes of anti-protons assuming design values of the beam parameters and without including the variations in bunch parameters. The multi-particle code BBSIM runs on parallel processors and includes the beam-beam interactions, and random dipole noise to mimic gas scattering. The simulation model in the results presented here assumed linear transport between the beam-beam interactions. More recently chromaticity sextupoles have been added to the model. Lifetimes were estimated by tracking $2x10^4$ particles through 10^6 turns and the bunch intensities were fitted to an exponential decay curve. Particles whose amplitudes exceed specified apertures are flagged so it is possible to estimate lifetimes as a function of the aperture.

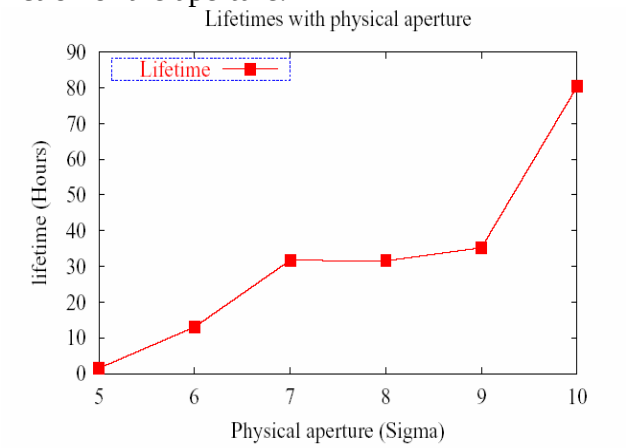

Figure 14: Lifetime of anti-proton bunch 1 calculated with BBSIM at collision as a function of the physical aperture.

The dependence of lifetime on the aperture is shown in Figure 14 for antiproton bunch 1. Figure 15 shows the relative lifetimes at 8 σ for 12 bunches normalized to the lifetime of bunch 1. The results using this model predict that the lifetime of anti-proton bunch 1 is significantly greater than that of the other bunches with only small variations between the other bunches. This lifetime pattern does not resemble either of the patterns seen in Figure 13. The discrepancies are due to several possible factors - the differences in bunch parameters need to be included, there is likely "cross-talk" between machine nonlinearities and beam-beam nonlinearities and the differences

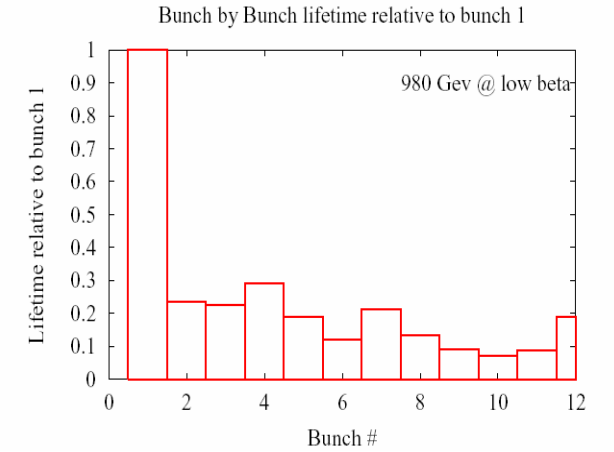

Figure 15: Relative lifetime of anti-proton bunches at collision from the code BBSIM.

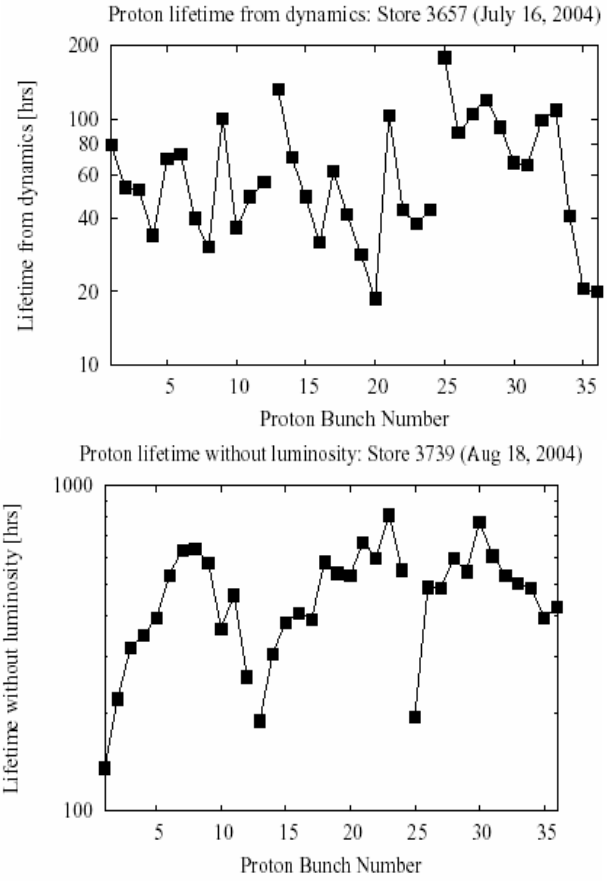

Figure 16: Dynamic proton lifetimes in two stores.

between the linear machine optics and the design optics used in the simulations.

The dynamic lifetimes of protons are shown in Figure 16 for the same two stores as in Figure 13. Again 3-fold symmetry is evident in the latter store but not in the earlier store. These dynamic lifetimes

also vary by roughly a factor of 10 between bunches. Intra-beam scattering has some influence on the dynamic lifetimes but cannot account for the observed variations given that proton bunch intensities and emittances are fairly uniform. We observe that beam-beam effects also have a strong influence on the protons. These losses are attributed mainly to the head-on interactions – after beams are brought to collision, proton losses are higher than anti-proton losses. Analysis shows that the non-luminous losses (losses not related to luminosity) of a proton bunch are greater if the vertical emittances of the colliding anti-proton bunches are smaller – seen in Figure 17.

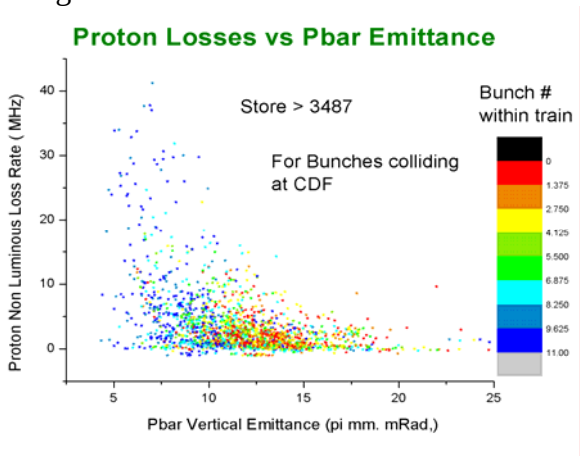

Figure 17: Correlation of proton non-luminous losses with the vertical emittance of the colliding anti-proton bunches (courtesy – P. Lebrun).

This phenomenon is qualitatively understood and has been observed previously at the SPS [16] and HERA [17]. Protons colliding with a smaller emittance anti-proton bunch experience the peak of the beam-beam force closer to the core of the proton bunch leading to larger losses. A quantitative explanation of this phenomenon is still lacking.

We end this section by a comment on longitudinal diffusion in the two beams. At the start of collisions, the longitudinal emittance of both beams is limited to under 4 eV-sec while the bucket area is 11 eV-sec. Intra-beam scattering leads to diffusion into larger portions of longitudinal phase space. Analysis by A. Tollestrup shows that while protons gradually fill the bucket, anti-protons stay confined to their initial area. Figure 18 shows the time evolution of the longitudinal density in a store as a function of the longitudinal action.

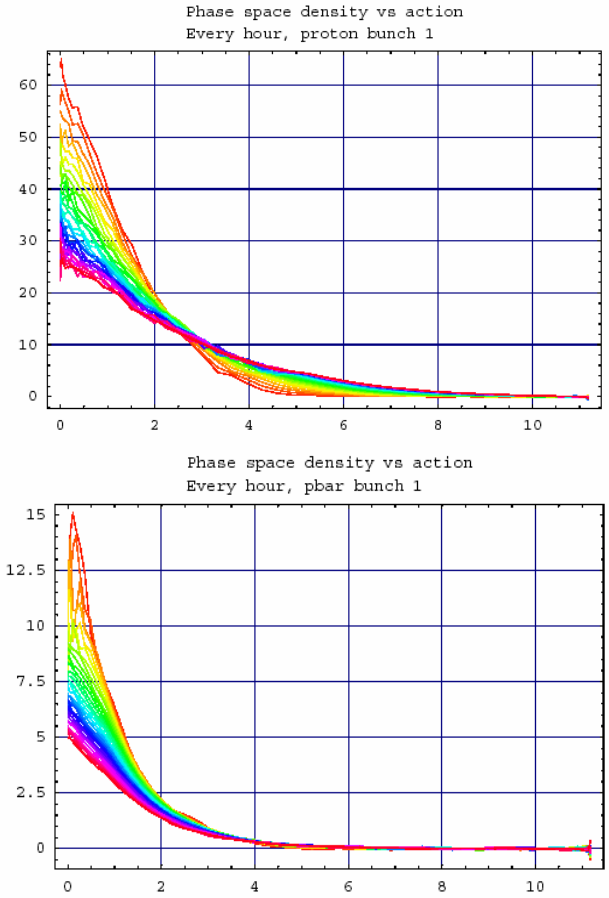

Figure 18: Evolution of the longitudinal density as a function of the longitudinal action. Top: protons, Bottom: anti-protons (courtesy: A.Tollestrup)

This suggests that the beam-beam interactions restrict the longitudinal DA of anti-protons to ~4 eV-sec but there is not a similar limit on the protons. This may be the first such observation of beam-beam imposed limitations on longitudinal dynamics.

Table 2 summarizes the recent beam-beam observations at Fermilab and the corresponding simulation activity. While this is a start, much more needs to be done.

Observations	Simulation	Comment
150 GeV		
Antiproton dynamic aperture	Yes	Agree at high chromaticity
Anti-proton lifetime	Yes	Depends on chromaticity
Ramp & Squeeze		
Losses during ramp	No	Simulations only at fixed energy
Losses during squeeze (2001-2002)	No	
980 GeV		
Impact of larger helices	Yes	Dynamic aperture only
Bunch by bunch tunes, orbits	Yes	Qualitatively good
Lifetimes, emittance growth	Yes	In progress
Proton losses at start of stores	No	No simulations of protons yet
Longitudinal dynamic aperture of anti-protons	No	Occurs on a long time scale
Tune scan of lifetimes	Yes	Limited tune scan of dynamic aperture
Cogging and IP scans	No	Limited benefit

Table 2: List of some important beam-beam observations, whether accompanied by simulations and comment on the simulations.

VI. RHIC

RHIC is a two-ring collider that has collided several species of ions. Data has been taken with collisions of gold on gold, deuterons on gold as well as protons on protons. Typically each bunch experiences 4 head-on collisions and 2 long-range interactions per turn. Beam-beam effects are observed to impact the emittance growth and lifetime. Simulations showed that the DA improves close to the SPS tunes and operation with polarized protons indeed showed better beam lifetime at these tunes [18]. At usual proton intensities, the beam-beam parameter is 0.004/IP although in some experiments with 2 head-on collisions, beam-beam parameters of 0.007/IP have been achieved.

Coherent modes driven by the beam-beam interactions have been observed when colliding proton beams of equal intensity. In a dedicated experiment with beams in collision only at a single IP and separated everywhere else, the mode frequencies were measured.

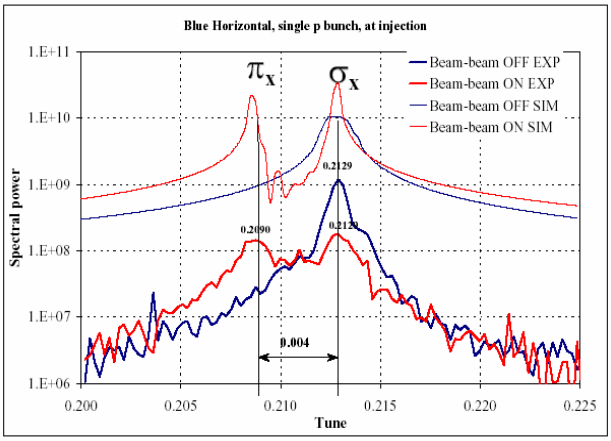

Figure 19: Measured and calculated coherent modes of protons in RHIC (Ref [19])

Strong-strong simulations using the code BBDEMO2C were also done with the appropriate beam parameters, reference [19]. Figure 19 shows a comparison of the measured and simulated bunch spectrum. Without collisions, no π mode was visible but the mode appeared when the

beams were colliding. The measured frequency split between the π mode and the σ mode was $\nu(\pi) - \nu(\sigma) = 1.3\xi$, in good agreement with the Yokoya parameter 1.31. The coherent mode frequencies calculated by BBDEMO2C were also in good agreement with the observed values.

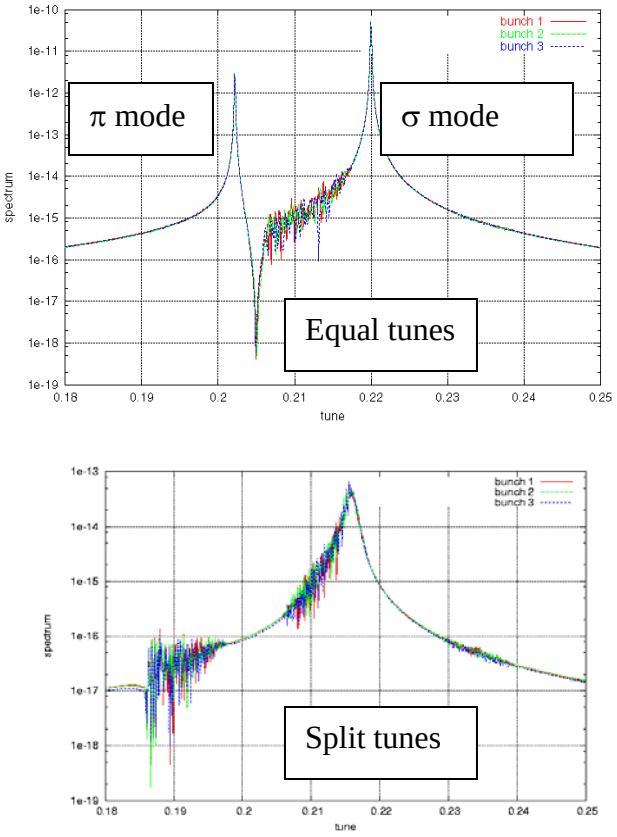

Figure 20: Bunch spectrum calculated with Beambeam3D showing the absence of the π mode when the tunes are split by more than ξ (courtesy: J. Qiang)

These coherent modes have not hurt machine performance so far. Usually a small tune split between the beams suffices to remove the π mode. This was predicted by A.Hofmann and has also been observed in simulations. Figure 21 shows the bunch spectrum calculated with the code Beambeam3D in two situations. In the first figure, both beams have the same tunes and in the second the tunes are moved apart by 0.02 while $\xi = 0.004$.

VII. LHC Beam-beam simulations

The LHC will be in a new regime where both long-range interactions and strong-strong effects will play a role. Considerable effort has been invested in simulations and analysis to understand the potential limitations. A comprehensive overview can be found in Reference [20]. The areas of effort include:

- Dynamic aperture due to beam-beam interactions and magnet field errors
- Orbits and tunes along the bunch trains
- Proper choice of crossing planes
- Beam-beam compensation with wires
- Impact of ground motion on emittance growth
- Impact of luminosity monitoring on emittance growth
- Excitation of synchro-betatron resonances
- Halo generation
- Possible loss of Landau damping and its restoration
- Alternative paths towards higher luminosity

Reference [20] should be consulted for more details about these studies. Here I'll focus on a few topics.

The weak-strong code WSDIFF has been used to examine diffusion generated by beam-beam interactions in several situations.

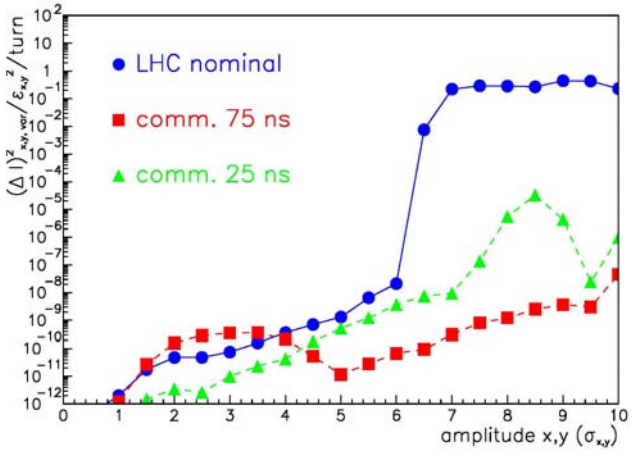

Figure 21: Diffusion rate with nominal beams and during commissioning with different bunch spacings and β* values, taken from Reference [20].

One example, seen in Figure 21, compares the diffusive dynamic aperture during nominal operation with that during commissioning with lower intensity bunches, different bunch spacing and higher β* values. At nominal parameters there is a sharp increase in the diffusion rate at 6σ while with the commissioning beam and 75nsec bunch spacing there is no such sharp increase. This predicts that the limitations due to the beam-beam interactions will not be severe during commissioning with these parameters. Another example shows the use of simulations in choosing parameters. The nominal plan calls for the beams crossing in the vertical plane at IP1 and in the horizontal plane at IP5. This results in a cancellation of the long-range tune shifts and perhaps other benefits. However calculation of the diffusive aperture with WSDIFF, seen in Figure 22, shows larger apertures when the crossing planes are chosen to be the same at both IPs. This topic is still under active investigation.

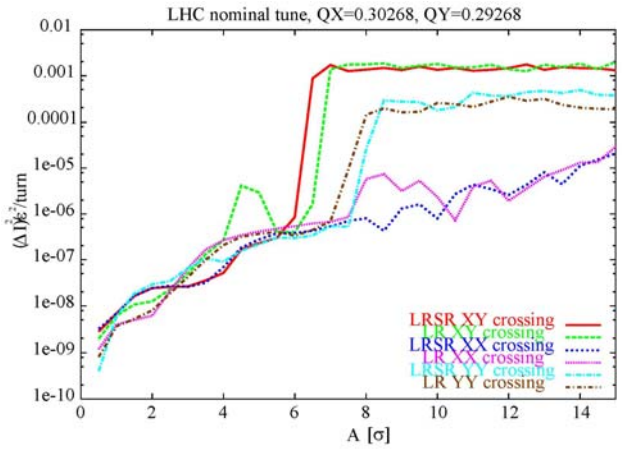

Figure 22: Diffusive dynamic aperture with different crossing schemes, Reference [20].

Compensation of the long-range interactions with current carrying wires is also under active investigation. In addition to simulation studies, beam studies have also been done at the SPS [21, 22]. Simulations with WSDIFF shown in Figure 23 found that a wire leads to a similar sharp diffusive aperture as due to the long-range interactions. These results were qualitatively confirmed during the first set of studies in the SPS.

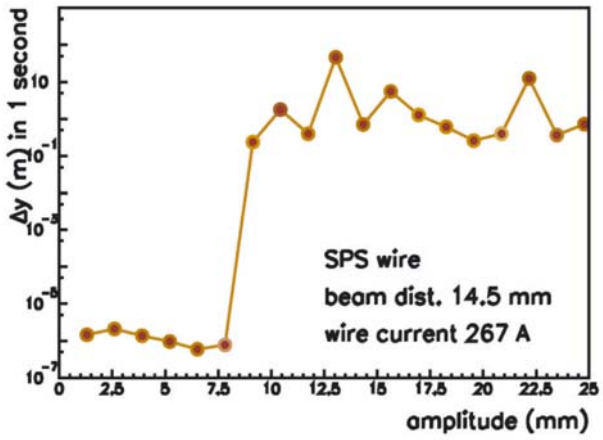

Figure 23: Diffusion rate due to a wire acting on a single beam, Reference [20].

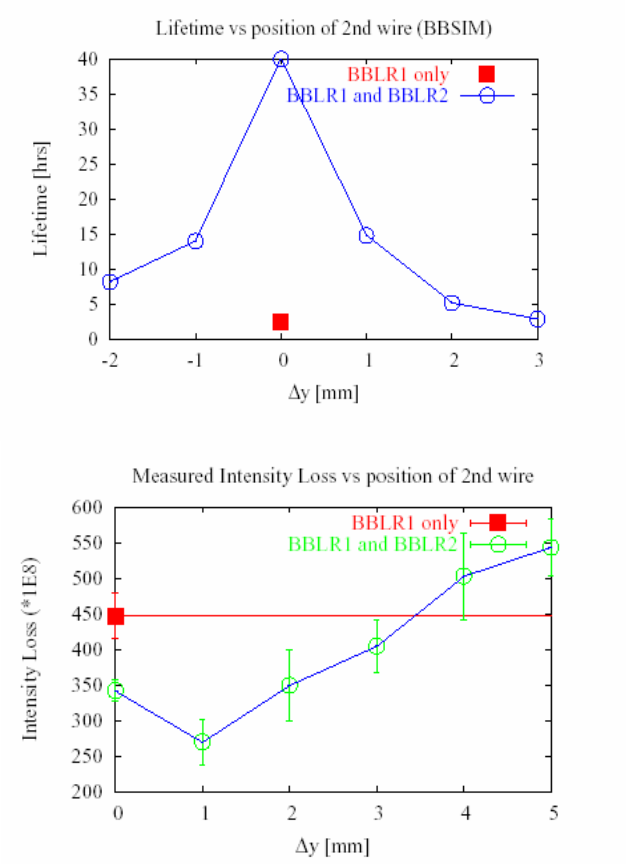

Figure 24: Alignment tolerance of the 2nd wire relative to the 1st wire – July 2004 studies [22]. Top: Measured intensity loss vs. the relative vertical displacement between the wires. Bottom: Calculated beam lifetime with BBSIM vs. the relative vertical displacement.

In a later set of studies performed in July 2004, the effect of one wire on the beam was compensated by another wire [22]. The alignment tolerance of the 2nd wire relative to the 1st wire was one of several measurements. In addition, simulations with the code BBSIM were also done prior to the experiments. The top plot in Figure 24 shows the measured beam intensity loss as the relative vertical alignment was changed. The smallest beam loss occurred with Δy = 1mm and not at Δy = 0, possibly due to a mis-calibration. The experiment showed that the compensation was not effective when the 2nd wire was offset by more than 3mm from the optimum position. The simulation showed that the beam lifetime had the same value (~ 2hrs) when the 2nd wire was offset by more than 2 mm as when the 2nd wire was absent, i.e. there was no compensation with an offset ≥ 2mm. Thus measurements and simulations were roughly consistent. Since then more wire compensation studies have been performed with further analysis and simulations in progress.

There has been a concern that the coherent modes in the LHC excited by the beam-beam interactions may not be Landau damped. The bunch spectrum has been calculated by several simulation codes with different approximations.

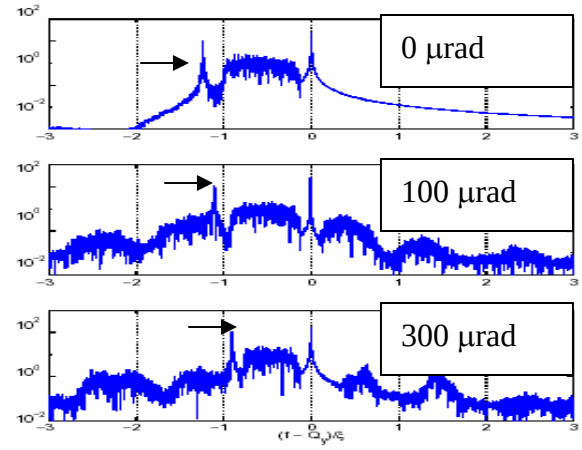

Figure 25: Bunch spectrum with the strong-strong code BEAMX showing the π mode at different crossing angles, Reference [11].

More recently a 6D parallelized code BEAMX was used to calculate the bunch spectrum for different crossing angles [11]. As seen in Figure 25, this simulation predicts that the π mode will be inside the continuum of modes at the full crossing angle of 300 μrad and probably not a source of concern.

VIII. SUMMARY

Beam-beam phenomena in hadron colliders have been studied for several decades now, yet new phenomena and limitations are observed as existing colliders are pushed to new regimes or new colliders are commissioned. The impact of long-range interactions has been strongly felt during Run II in the Tevatron. We have learnt again that beam-beam performance cannot be characterized by the beam-beam tune shift alone. Several other parameters such as the chromaticity, beam separations around the ring, mismatched emittances as well as the usual suspects: tunes and coupling, determine how the beam-beam interactions limit beam quality. Until recently simulations were mostly used to calculate quantities that are not often measured such as dynamic apertures and tune shifts with amplitude. However the wide availability of parallel computers and fast algorithms now make calculations of emittance growth and lifetimes feasible in many situations. Experience has shown that it is important to include an accurate fully six dimensional model of the linear optics in the simulation model. We still have to make judicious choices about the other beam physics effects (rest-gas scattering, intra-beam scattering, magnetic nonlinearities, impedances, power supply ripple and fluctuations etc.) to include in the simulation model. The simulation results presented here for the Tevatron, RHIC and the SPS are consistent with measurements in some cases. The next step for the case of Tevatron simulations will be to demonstrate a qualitative agreement between simulated bunch-by-bunch lifetimes and emittances and measurements. Beam-beam simulations will have come of age when we can

use them routinely to improve the performance of a collider.

ACKNOWLEDGEMENTS

I thank W. Fischer, W. Herr, A. Kabel, J.P. Koutchouk, P. Lebrun, J. Qiang, F. Schmidt, A. Tollestrup, A. Valishev, M. Vogt, and F. Zimmermann for useful discussions and generous use of their results.

REFERENCES

[1] G. Hoffstaetter, M. Vogt and F. Willeke, ICFA Beam Dynamics Newsletter, April 2003, page 7
[2] BBSIM web page:
http://waldo.fnal.gov/~tsen/BBCODE/public
[3] D. Shatilov, Part. Acc. **52**, 65, 1996
[4] A. Kabel et al, PAC03 Proceedings, page 3542
[5] J. Qiang et al., PAC03 Proceedings, page 3401
[6] MAD web page:http://mad.home.cern.ch/mad/
[7] Sixtrack web page: http://frs.home.cern.ch/frs/
[8] Tevlat, written by A. Russell and N. Gelfand, FNAL
[9] M. Vogt, T. Sen and J. Ellison, PRSTAB 5, 24401 (2002)
[10] Y. Papaphilippou and F. Zimmermann, PRSTAB 2, 104001 (1999)
[11] F.W. Jones and W. Herr, PAC03 Proceedings, page 3404
[12] T. Sen, ICFA Beam Dynamics Newsletter, August 2004, page 45
[13] R. Pasquinelli et al, PAC03 Proceedings, page 3068
[14] T. Sen, B. Erdelyi, M. Xiao and V. Boocha, PRSTAB, 041001 (2004)
[15] V. Shiltsev, EPAC 2004 Proceedings, page 239
[16] K. Cornelis, M. Meddahi and R. Schmidt, EPAC90 Proceedings, page 1670
[17] R. Brinkmann and F. Willeke, PAC93 Proceedings, page 3742
[18] W. Fischer and R. Tomas, ICFA Beam Dynamics Newsletter, August 2004, page 58
[19] M. Vogt, et al. EPAC 2002 Proceedings page 1428
[20] F. Zimmermann, ICFA Beam Dynamics Newsletter, August 2004, page 26
[21] J.P. Koutchouk, J. Wenninger and F. Zimmermann, EPAC 2004 Proceedings, page 1936
[22] J.P. Koutchouk et al. to be published